Electronic Supplementary Information (ESI)

Graphene Oxide-Fullerene Nanocomposite Laminates for Efficient Hydrogen Purification

Qi Guo,[a] Behnam Ghalei,*[ab] Detao Qin,[ab] Daizu Mizutani,[a] Ikumi Joko,[ab] Habib Al-Aziz,[ab] Tomohiro Higashino,[a] Masateru M Ito,[ab] Hiroshi Imahori,*[abc] and Easan Sivaniah*[ab]

[a]Department of Molecular Engineering, Graduate School of Engineering, Kyoto University, Kyoto, 615-8510, Japan
[b]Institute for Integrated Cell-Material Sciences (iCeMS), Kyoto University, Kyoto, 606-8501, Japan
[c]Institute for Liberal Arts and Sciences (ILAS), Kyoto University, Kyoto, 606-8316, Japan

1. Materials and methods

1.1 Chemicals

Alfa Aesar provided graphite flakes, and SES Research supplied fullerene (99.95%, powder). N-methyl glycine, paraformaldehyde, anhydrous sodium sulfate, methyl iodide, 1-methyl-piperazine, sulfuric acid, phosphoric acid, potassium permanganate, hydrochloric acid, hydrogen peroxide solution, toluene, and ethyl acetate were purchased from Wako Pure Chemical Industries and used as received.

1.2 Characterization

^{1}H NMR spectra were recorded using a JEOL ECZ-400 spectrometer (operating at 400 MHz), with $CDCl_3$ as the solvent ($CDCl_3$: δ = 7.26 ppm). High-resolution mass spectra were measured on an LTQ orbitrap XL (MALDI). UV-vis-near-infrared absorption spectra were obtained using a Perkin Elmer Lambda 900 UV/vis/NIR spectrometer. X-ray diffraction (XRD) patterns were measured by wide-angle XRD (Rigaku RINTXRD, Japan) in the range of 5° to 40° at a scan rate of 10°/min using Cu K-α1 radiation at a voltage of 40 kV and a current of 200 mA (K radiation wavelength is 1.54056 Å). The zeta potential was measured using the Malvern Zetasizer Nanoinstrument (Malvern Panalytical Ltd.). The nanoparticle size distribution was measured using the dynamic light scattering (DLS) technique with a nanoparticle analyzer SZ-100. The field emission scanning electron microscope (FESEM) instrument (Hitachi S-4800) was used to examine the morphology of membranes and to determine the thickness of the selective layer of the membrane. The samples were freeze-fractured in liquid nitrogen and sputtered with osmium to prevent electron charging. X-ray photoelectron spectroscopy (XPS) measurements were obtained using an X-ray photoelectron spectrometer (ESCA-3400, Shimadzu).

1.3 Synthesis of C_{60} derivatives

f1. Compound **f1** was prepared under modified conditions of a literature procedure[1]. A mixture of C_{60} (220 mg, 0.3 mmol), N-methyl glycine (54 mg, 0.6 mmol), and paraformaldehyde (46 mg, 1.5 mmol) was heated overnight at reflux in 400 mL toluene under argon. The resulting brown solution was washed with water, dried over Na_2SO_4, and concentrated under reduced pressure. The crude product was purified by flash chromatography on silica gel (eluent: toluene and then toluene/triethylamine 100:1), yielding 66.8 mg (29%) of the mono adduct (N-methyl pyrrolidine)-C_{60} (^{1}H NMR δ = 4.42 (s, 4H), 3.14 (s, 6H)) and 119.5 mg (48%) bisadducts. (N-methyl pyrrolidine)-C_{60} (120.0 mg, 0.1543 mmol) was dissolved in methyl iodide (15 mL)

and stirred for 72 h at room temperature to yield a brown residue. The precipitate was filtrated and then washed with toluene to yield a red-brownish powder (141.4 mg, 99.6%). ESI-MS found: m/z = 794.0975 for $[C_{64}H_{12}N + H]^+$, calcd 795.1048.

f2. Compound **f2** was synthesized according to a previously reported method[2]. Four bis(N-methylpyrrolidine-C_{60}) isomers obtained from the above reaction can be separated by column chromatography using toluene/EtOAc = 10:1 as an eluent. They can be classified as bisadducts trans-2, trans-3, trans-4, and cis-3[3]. ^{1}H NMR (400 MHz, $CDCl_3$) of trans-2: δ = 4.64 (d, 2H), 4.46 (d, 2H), 4.34 (t, 4H), and 3.03 (s, 6H). Trans-2 (30 mg, 0.0359 mmol) was dissolved in methyl iodide (15 mL) and stirred for 72 h at room temperature to yield a brown residue. The precipitate was filtrated and then washed with toluene to yield a red-brownish powder (31 mg, 79.1%). ESI-MS found: m/z = 865.1685 for $[C_{68}H_{20}N_2 + H]^+$, calcd 865.1705.

f5. Compound **f5** was synthesized according to a previously reported method[4]. Hexachlorofullerene $C_{60}Cl_6$ (100 mg) was dissolved in 300 mL toluene under continuous stirring. Then, 1-methyl-piperazine (64.6 mg, 6 eq) was added dropwise into the solution, stirring the mixture for another 1 h. The precipitate was collected by centrifugation and washed with toluene to yield a brown powder (46.2 mg). ^{1}H NMR (400 MHz, $CDCl_3$) of **f5**: δ = 3.21 (s, 20H), 2.75 (s, 20H), and 2.40 (s, 15H). ESI-MS found: m/z = 1233.4798 for $[C_{85}H_{56}N_{10} + H_2O]^+$, calcd 1233.4689.

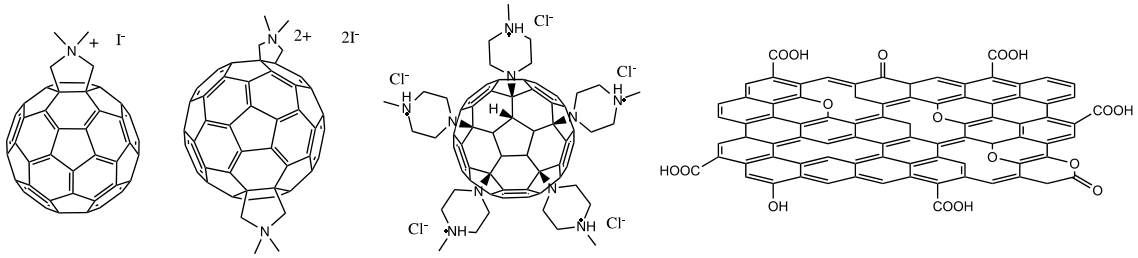

Fig. S1. Structures of fullerene derivatives and GO investigated in this study

1.4 Synthesis of GO

Single-layered GO was synthesized using the improved hummers' method[5]. In an ice bath, graphite powder (1 g) was added to a 9:1 mixture of concentrated H_2SO_4/H_3PO_4 (120:13.3 mL) in an ice bath and stirred for 20 min. Then, 6 g $KMnO_4$ was gradually added to the reaction media, and the mixture was stirred at 50 °C for 4 h. The reaction was cooled to room temperature and poured slowly into 150 mL cold water (0°C -2°C), then 2 mL H_2O_2 (30%) was added dropwise to change the solution color to light yellow. The product was filtered with 10% aqueous HCl and thoroughly washed with distilled water until the pH reached 7. The average size of the synthesized GO sheets is estimated to be about 2 μm, determined by DLS measurement, as shown in section 4 "*Properties of synthesized GO sheets and GO-C_{60} membrane*" of this ESI.

1.5 Preparation of GO-C_{60} derivatives membranes

The GO dispersion was exfoliated by sonication and centrifuged at 5000 rpm for 30 min to remove large flakes. The supernatant was then centrifuged at 10000 rpm for 30 min to remove small flakes. The precipitate was diluted to about 0.1 mg/mL and sonicated for 10 min to have the GO stock solution. Fullerene derivative solution was centrifuged at 8000 rpm for 30 min to remove undissolved sediments and then diluted to about 0.1 mg/mL to have the stock solution. For making the nanolaminate membranes, the concentration of GO was varied from 0.0033 to 0.01 mg/ml, while the ratio of C_{60} derivative over GO was varied from 5%, 10%, to 20%. A mixture of GO and C_{60} derivative solution was sonicated for 10 minutes in an ice bath. Afterwards,

the mixture solution was vacuum filtrated at a vacuum pressure of 10 Pa through the anodic aluminum oxide (AAO) filters (purchased from Whatman ™) with an average pore size of 20 nm.

1.6 Gas permeation tests

Gas permeation measurements were conducted using a homemade membrane permeation/separation unit (see Figure S6, ESI). The Wicke-Kallenbach cell was used to measure the gas permeation properties of the fabricated membranes. The edges of the membrane disks were covered with tape coated with a silicone rubber pad before starting the measurements to prevent damage to the selective layer. Mass flow controllers maintained the volumetric flow rate of feed gases at 100 mL min^{-1} for the mixed gas (H_2: CO_2 = 1: 1, v/v). Argon was used as the sweep gas at a constant volumetric flow rate of 50 mL min^{-1} to eliminate concentration polarization on the permeate side. A calibrated gas chromatograph (Shimadzu GC-2014) was used to analyze the composition of the permeate gas. The gas permeances and selectivity in this work are reported based on the average values of three separate measurements of different membrane samples.

2. Properties of synthesized C_{60} derivatives

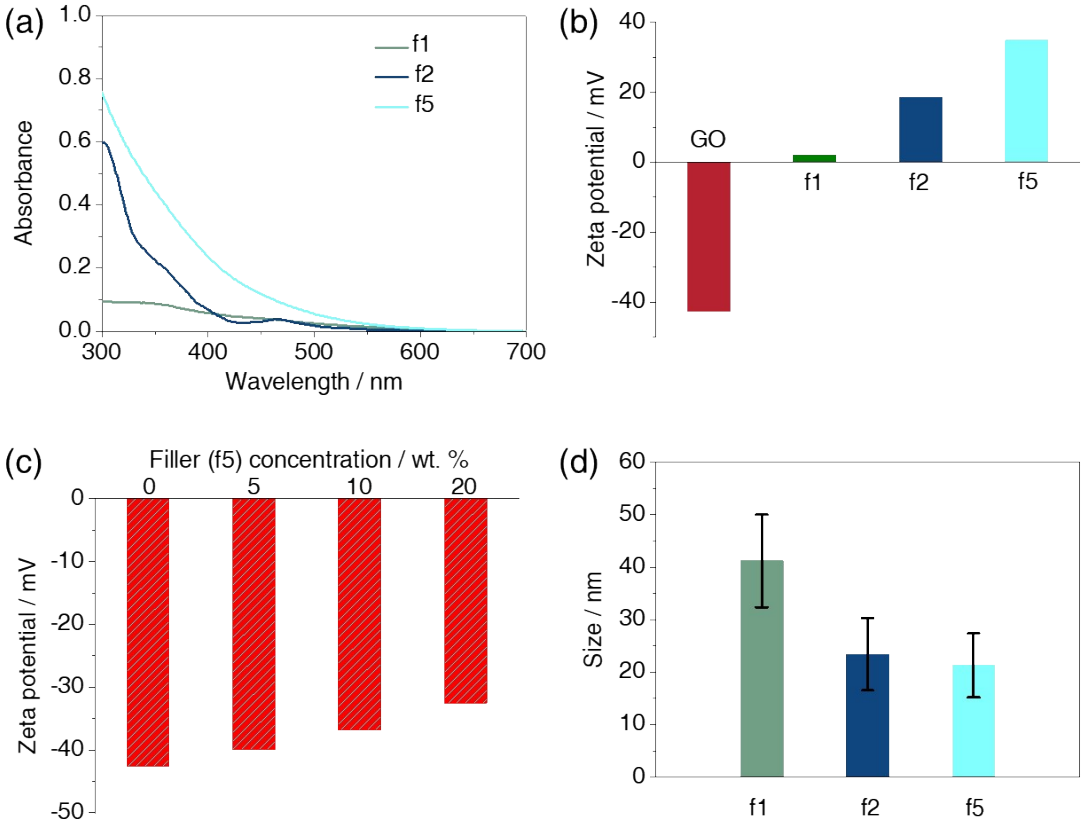

Fig. S2. (a) UV-vis absorption spectra of f1 (0.1 mg/mL), f2 (0.1 mg/mL), and f5 (0.1 mg/mL) solutions. Zeta potential values of (b) C_{60} derivatives solutions and (c) GO-f5 solutions with different f5 concentrations. (d) Size distribution of f1, f2, and f5 nanoparticle clusters in 0.1 mg/mL solution, measured by dynamic light scattering (DLS). The concentrations of C_{60} derivatives to measure DLS are 0.1 mg/ml, which is significantly higher than their concentrations to make the nanolaminate membranes.

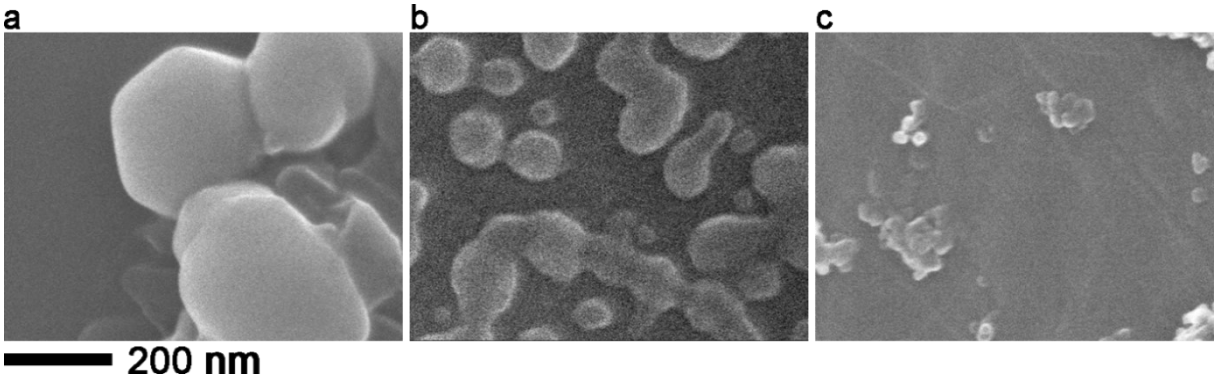

Fig. S3. SEM images of the (a) f1, (b) f2, and (c) f5 nanoparticle clusters. C_{60} aqueous solutions were cast on a silicon wafer to prepare the samples. The concentration of C_{60} derivatives to prepare the solution is 0.1 mg/ml, which is significantly higher than their concentrations to make the nanolaminate membranes. SEM pictures were taken after the drying of the samples, while the drying process aggravates the aggrevation of nanoparticles. The SEM results demonstrate the same trend as the DLS analysis: nanoparticle cluster sizes follow the order f1 > f2 > f5, indicating f5 and f2 have better dispersibility than f1.

3. XRD analysis

The interlayer spacing of GO sheets can be derived from the scattering angle (θ) by the following equation:

$$d = \lambda / (2 \sin\theta)$$

where d indicates the interlayer spacing, λ is 1.54056 Å (wavelength of copper target), and θ is the scattering angle.

Table S1. Parameters for XRD measurements of different membrane samples

	2 θ (°)	**Interlayer spacing (Å)**
GO	10.06	8.79
GO + 2% f5	9.70	9.11
GO + 5% f5	9.04	9.77
GO + 10% f5	9.50	9.30
GO + 20% f5	9.68	9.13

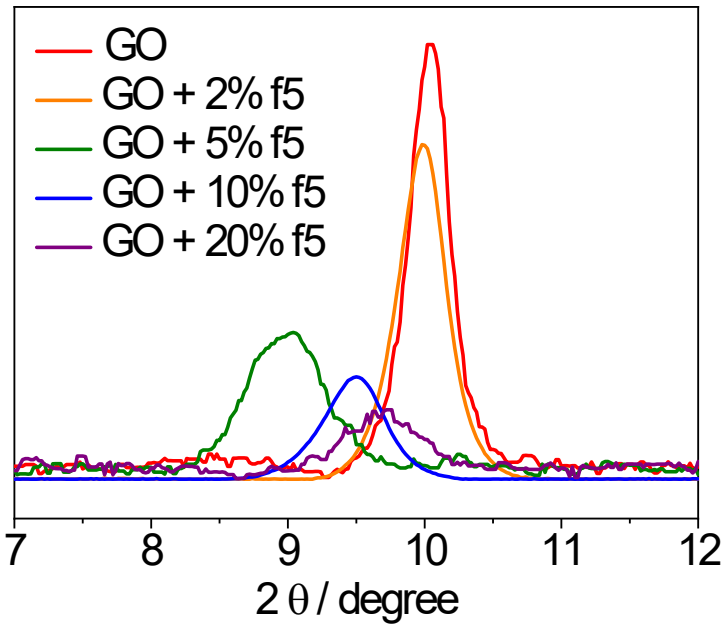

Fig. S4. XRD patterns of membranes with different f5 filler concentrations, and the peak position and interlayer spacing parameters of the samples are listed in Table S1.

4. Properties of synthesized GO sheets and GO-C_{60} membranes

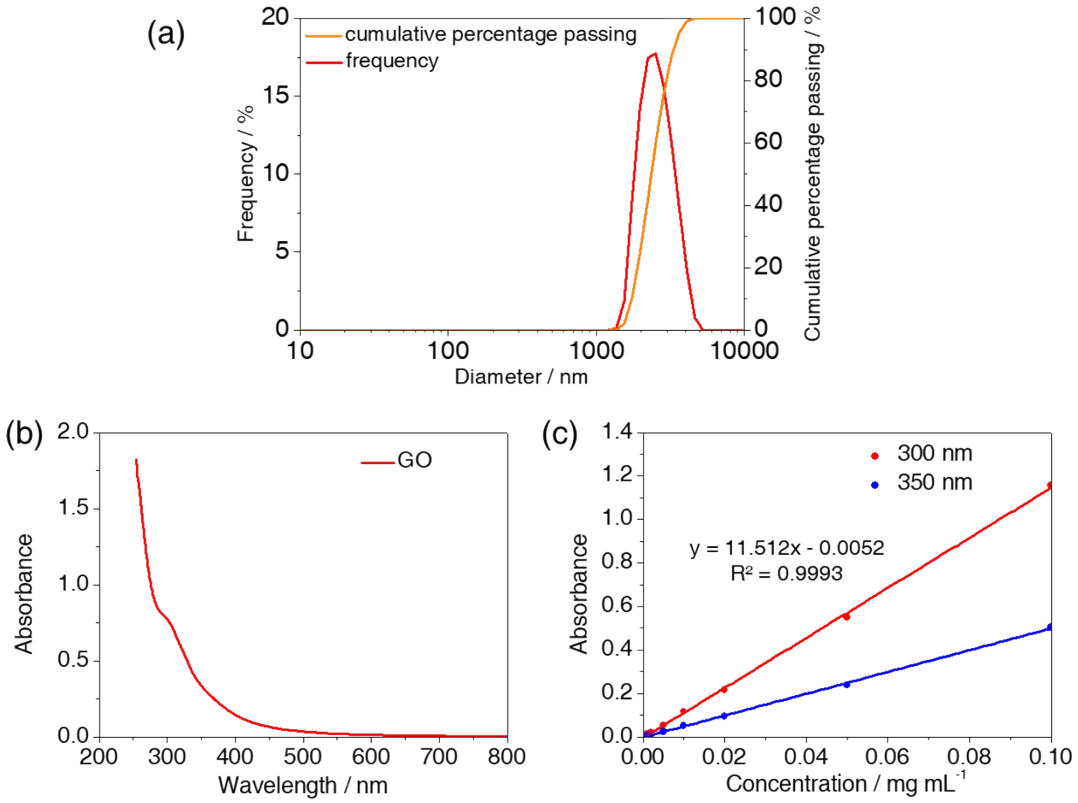

Fig. S5. (a) Size distribution of GO sheets in solution by DLS. (b) UV-visible absorption spectrum of GO solution. (c) The linear relationship between GO solution concentration and absorbance at 300 nm and 350 nm. The concentration of GO solution can be calculated from the absorbance at 300 nm.

5. Basic introduction of gas separation tests

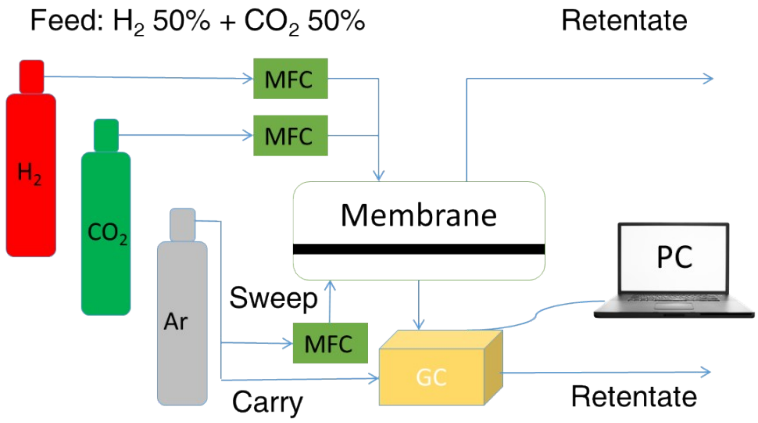

Fig. S6. Apparatus Scheme for Gas Separation unit. MFC: Mass flow controller. GC: Gas chromatography.

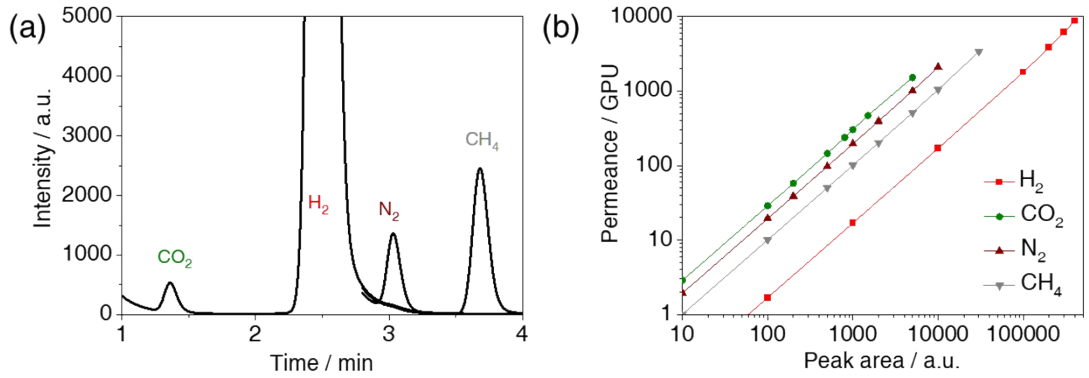

Fig. S7. (a) A curve acquired from GC. CO_2, H_2, N_2, and CH_4 peaks appear at the 1.25-1.5, 2.25-2.75, 2.90-3.20, and 3.50-3.90 min, respectively. (b) Relationship between peak area and gas permeance. GPU: gas permeance unites, 1 GPU = 3.35×10^{-10} mol m^{-2} s^{-1} Pa^{-1}. Selectivity (α)= Permeance (H_2) / Permeance (CO_2, N_2, or CH_4).

6. XPS Analysis

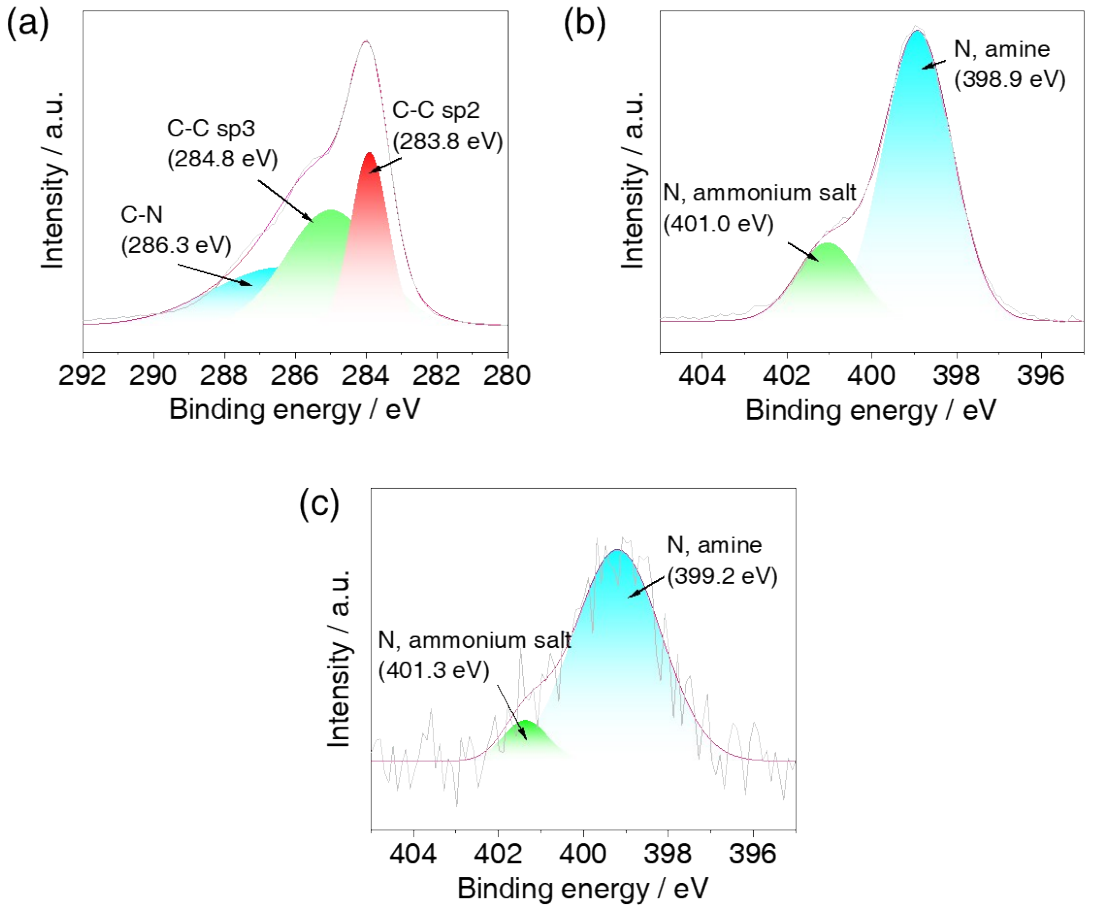

Fig. S8. (a, b) XPS C 1s and N 1s scanning spectra of f5, respectively. (c) XPS N 1s scanning spectra of GO-f5 membrane. In XPS spectra, the scanning line and fitting line are shown in grey and pink, respectively. In addition, as shown in the Fig. 2 of main text, the XPS C 1s scanning spectrum of the as-synthesized GO shows carboxyl and hydroxyl groups, providing good solubility and negatively charged single GO layers in water. When positively charged C_{60} derivative f5 is added to the GO membrane, the intensity of the C=O, O-C=O, and C-O peaks significantly decreases, indicating that GO and f5 interact via hydrogen bonds or electrostatic attraction.

7. SEM images of membranes with different thickness

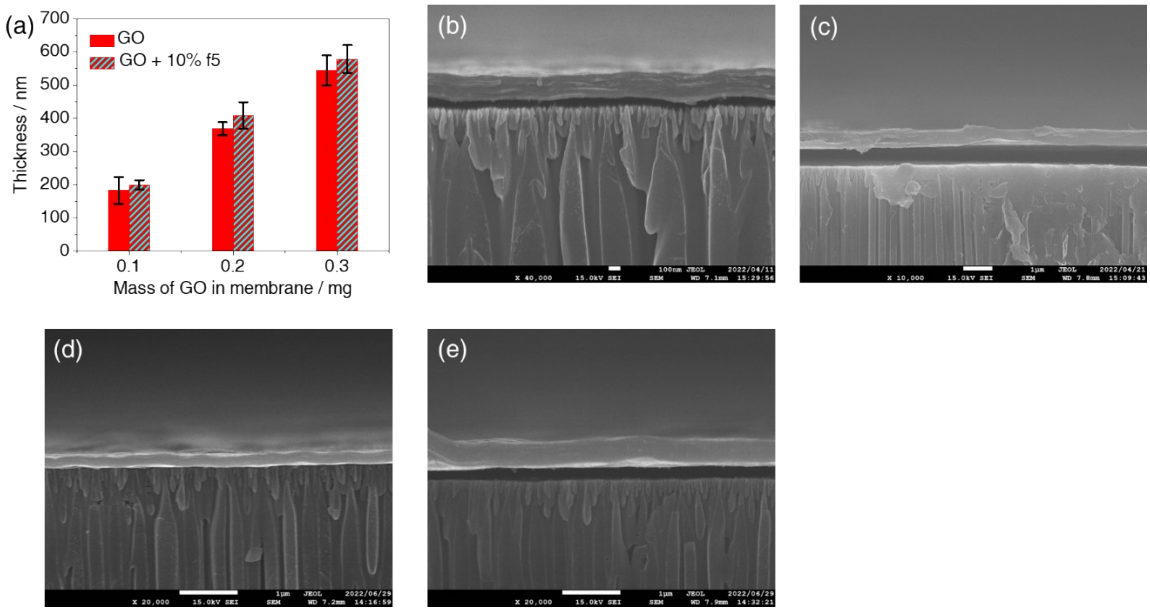

Fig. S9. (a) Selective layer thicknesses for GO and GO-f5 membranes, which are estimated from SEM images. Cross-section SEM images for (b: GO 0.1 mg; c: GO 0.1 mg + 10% f5; d: GO 0.3 mg; e: GO 0.3 mg + 10% f5).

8. Equimolar mixture gas permeances (GPU) and separation factors

Table S2. Equimolar H_2 and CO_2 mixture gas permeances and separation factors (α) for GO-f5 membranes with different filler concentrations.

	m(GO) / mg	m(f5) / mg	H_2 permeance / GPU	CO_2 permeance / GPU	$\alpha(H_2/CO_2)$
AAO	0	0	9106.7±76	1060.8±52	8.5±0.3
GO-f5 5%	0.1	0.00526	4591.9±327	110.8±7	41.4±2.8
GO-f5 10%	0.1	0.0111	4195.7±176	76.9±5	54.5±1.4
GO-f5 20%	0.1	0.025	4749.4±120	97.7±4	48.6±0.9

Table S3. Equimolar H_2 and CO_2 mixture gas permeances and separation factors for GO membranes with different thicknesses.

	m(GO) / mg	m(f5) / mg	H_2 permeance / GPU	CO_2 permeance / GPU	$\alpha(H_2/CO_2)$
AAO	0	0	9106.7±76	1060.8±52	8.5±0.3
GO	0.1	0	5407.6±250	200.3±32	27.2±3.5
GO	0.2	0	4101.9±262	127.8±25	32.4±3.8
GO	0.3	0	2568.5±280	42.1±9.9	62.0±9.2
GO	0.4	0	870.0±30	-	-

Table S4. Equimolar H_2 and CO_2 mixture gas permeances and separation factors for GO-f5 membranes with different thicknesses.

	m(GO) / mg	m(f5) / mg	H_2 permeance / GPU	CO_2 permeance / GPU	$\alpha(H_2/CO_2)$
AAO	0	0	9106.7±76	1060.8±52	8.5±0.3
GO-f5 10%	0.1	0.0111	4195.7±176	76.9±5	54.5±1.4
GO-f5 10%	0.2	0.0222	3370.5±158	57.0±4	59.2±3
GO-f5 10%	0.3	0.0333	2585.2±263	34.3±2	75.3±4
GO-f5 10%	0.4	0.0444	541.3±87	-	-

Table S5. Equimolar H_2 and CO_2 mixture gas permeances and separation factors for GO-C_{60} derivative membranes with different fillers.

	m(GO) / mg	m(filler) / mg	H_2 permeance / GPU	CO_2 permeance / GPU	$\alpha(H_2/CO_2)$
GO + 10% f5	0.2	0.0222	3370.5±158	57.0±4	59.2±1.9
GO + 10% f2	0.2	0.0222	3863.2±82	85.4±1	45.2±1.4
GO + 10% f1	0.2	0.0222	3918.4±207	109.0±5	35.9±1.2
GO + 10% C_{60}	0.2	0.0222	4265.8±190	125.1±16	34.3±3.1
GO	0.2	0	4101.9±262	127.8±25	32.4±3.8

9. Additional discussion on the separation performance of GO-f1, GO-f2, and GO-$C_{60,p}$ membranes.

We also developed composite membranes using other types of C_{60} derivatives, *i.e.* f1 and f2 as well as pristine fullerene ($C_{60,p}$). Membrane samples containing 0.2 mg GO and 10% f1 or f2 were tested using the same experimental procedure (Fig. 4a). The GO-f2 membranes have higher H_2/CO_2 selectivity than GO membranes but lower selectivity than GO-f5 membranes. It was found that the zeta potential of f2 fillers was lower than that of f5. Therefore, we speculated that the lower H_2/CO_2 selectivity in f2-containing membranes might be due to its lower neutralization capacity and defect-sealing ability between GO nanosheets. The gas permeance and selectivity of GO-f1 and GO-$C_{60,p}$ are comparable to those of pure GO membranes, primarily due to the low solubility and low zeta potential of f1 and $C_{60,p}$. These results prove that the solubility and charge amounts of C_{60} derivatives significantly impact the gas separation ability of GO-filler membranes.

10. A summary of the H_2/CO_2 separation performance of various membranes

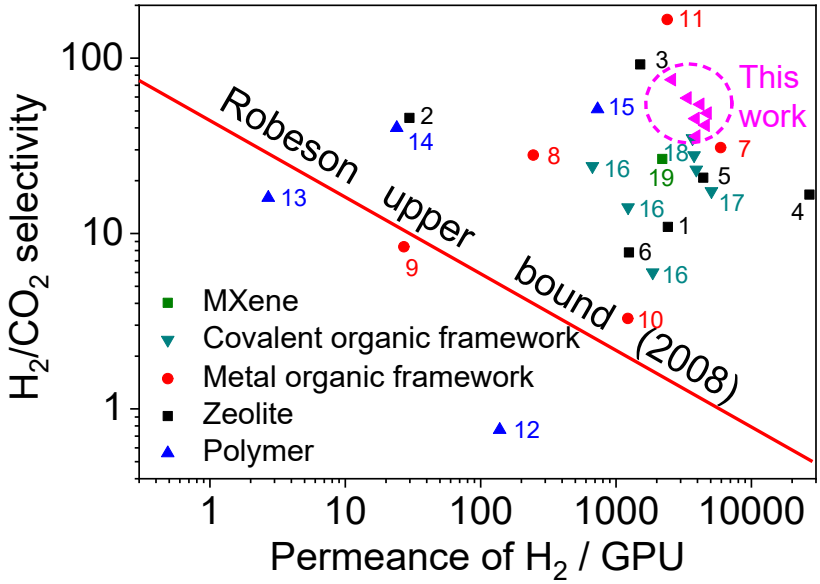

Fig. S10. H_2/CO_2 selectivity as a function of H_2 permeance for GO-C_{60} derivatives membranes in this work, compared with literature data.

Table S6. A summary of the H_2/CO_2 separation performance of various membranes.

Number in Fig. S10	Membrane materials	H_2 permeance (GPU)	Selectivity (H_2/CO_2)	Reference
1	Zeolite	2417.91	10.9	6
2		29.8	45.6	7
3		1510.44	92	8
4		26865.6	16.66	9
5		4417.91	20.8	10
6		1247.7	7.8	11
7	Metal organic framework	5925.3	30.9	12
8	(MOF)	244.77	28	13
9		27.1	8.4	14
10		1223.8	3.28	15
11		2388	166	16
12	Polymer	138.2	0.76	17
13		2.7	16	18
14		24	40	19
15		730.5	51.2	20
16	Covalent organic framework	1866.8	6	21
	(COF)	1227.6	14.1	
		669.1	24.2	
17		5074.6	17.4	22
18		3671.1	34.9	23
		3920.1	23.1	
		3772.7	27.9	
19	MXene (as an example)	2200	26.6	24

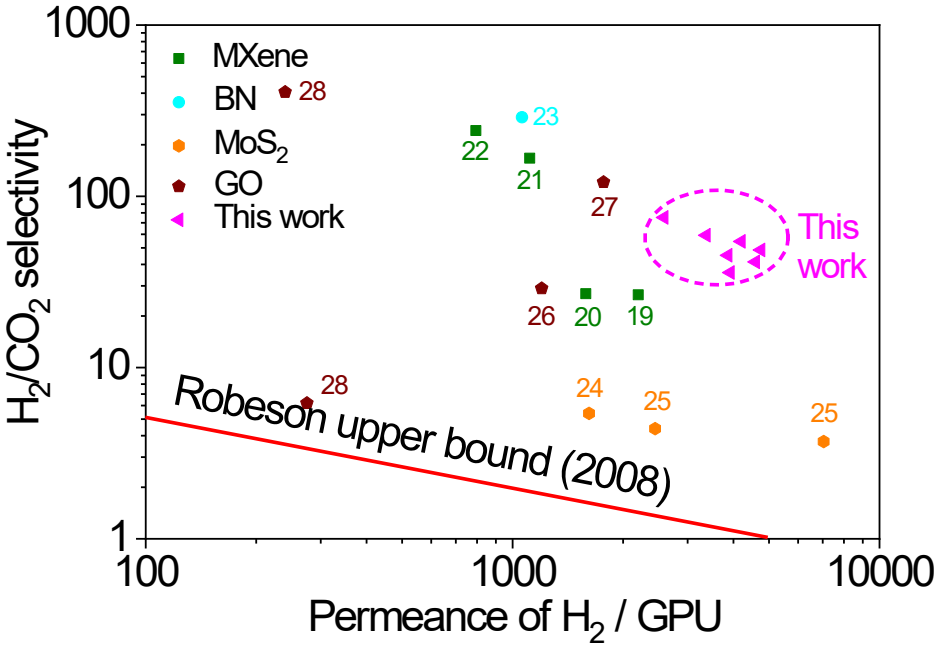

Fig. S11. The comparison of this study with other 2D nanomaterial based membranes.

Table S7. The H_2/CO_2 separation performance of various 2D nanosheet membranes in literature.

Number in Fig. S11	Membrane materials	H_2 permeance (GPU)	Selectivity (H_2/CO_2)	Reference
19	MXene	2200	26.6	24
20		1584	27	25
21		1113.3	167	26
22		794.02	242	27
23	BN	1061.3	289.5	28
24	MoS_2	1615.38	5.4	29
25		2446	4.4	30
		7044	3.7	
26	GO	1200	29	31
27		1770.14	121	32
28		275	6.2	33
		240	406	

11. The separation of H_2/N_2 and H_2/CH_4 gas mixtures

Table S8. Equimolar H_2 and N_2 mixture gas permeances and separation factors for GO and GO-f5 membranes.

	m(GO) / mg	m(f5) / mg	H_2 permeance / GPU	N_2 permeance/ GPU	$\alpha(H_2/N_2)$
AAO	0	0	7433.3±120	1828.9±102	4.0±0.2
GO	0.2	0	3067.9±29	293.5±6	10.4±0.3
GO + 10% f5	0.2	0.0222	2681.6±52	155.8±8	17.2±1.2

Table S9. Equimolar H_2 and CH_4 mixture gas permeances and separation factors for GO and GO-f5 membranes.

	m(GO) / mg	m(f5) / mg	H_2 permeance / GPU	CH_4 permeance / GPU	$\alpha(H_2/CH_4)$
AAO	0	0	9176.0±192	2437.7±83	3.7±0.1
GO	0.2	0	4361.3±88	293.5±18	9.2±0.2
GO + 10% f5	0.2	0.0222	3306.2±226	203.0±7	16.3±1.7

[1] A. M. Cassell, C. L. Asplund and J. M. Tour, *Angew. Chem. Int. Ed.,* 1999, **38**, 2403.
[2] T. Mashino, N. Usui, K. Okuda, T. Hirota and M. Mochizukia, *Bioorg. Med. Chem.,* 2003, **11**, 1433.
[3] Q. Lu, D. I. Schuster and S. R. Wilson, *J. Org. Chem.,* 1996, **61**, 4764.
[4] A. B. Kornev, E. A. Khakina, S. I. Troyanov, A. A. Kushch, A. Peregudov, A. Vasilchenko, D. G. Deryabin, V. M. Martynenko and P. A. Troshin, *Chem. Commun.,* 2012, **48**, 5461.
[5] W. S. Hummers and R. E. Offeman, *J. Am. Chem. Soc.,* 1958, **80**, 1339.
[6] X. Li, K. Li, S. Tao, H. Ma, R. Xu, B. Wang, P. Wang and Z. Tian, *Microporous Mesoporous Mater.*, 2016, **228**, 45.
[7] Z. Hong, F. Sun, D. Chen, C. Zhang, X. Gu and N. Xu, *Int. J. Hydrog. Energy*, 2013, **38**, 8409.
[8] K. P. Dey, D. Kundu, M. Chatterjee and M. K. Naskar, *J. Am. Ceram. Soc*., 2013, **96**, 68.
[9] F. Zhang, X. Zou, X. Gao, S. Fan, F. Sun, H. Ren and G. Zhu, *Adv. Funct. Mater.*, 2012, **22**, 3583.
[10] J. K. Das and N. Das, *ACS Appl. Mater. Interfaces,* 2014, **6**, 20717.
[11] A. Huang, J. Caro, *Chem. Commun.*, 2010, **46**, 7748.
[12] F. Zhang, X. Zou, X. Gao, S. Fan, F. Sun, H. Ren and G. Zhu, *Adv. Funct. Mater.*, 2012, **22**, 3583.
[13] N. Wang, A. Mundstock, Y. Liu, A. Huang and J. Caro, *Chem. Eng. Sci.*, 2015, **124**, 27.
[14] Y. Li, H. Bux, A. Feldhoff, G. Li, W. Yang and J. Caro, *Adv. Mater.,* 2010, **22**, 3322.
[15] K. Huang, Z. Dong, Q. Li and W. Jin, *Chem. Commun.*, 2013, **49**, 10326.
[16] Y. Peng, Y. Li, Y. Ban and W. Yang, *Angew. Chem. Int. Ed.*, 2017, **56**, 9757.
[17] M. Carta, R. Malpass-Evans, M. Croad, Y. Rogan, J. C. Jansen, P. Bernardo, F. Bazzarelli, N. B. McKeown, *Science,* 2013, **339**, 303.
[18] L. Zhu, M. T. Swihart and H. Lin, *Energy Environ. Sci.*, 2018, **11**, 94.
[19] M. Shan, X. Liu, X. Wang, I. Yarulina, B. Seoane, F. Kapteijn and J. Gascon, *Sci. Adv.*, 2018, **4**, eaau169.
[20] B. Ghalei, Y. Kinoshita, K. Wakimoto, K. Sakurai, S. Mathew, Y. Yue, H. Kusuda, H. Imahori and E. Sivaniah, *J. Mater. Chem. A*, 2017, **5**, 4686.
[21] H. Fan, A. Mundstock, A. Feldhoff, A. Knebel, J. Gu, H. Meng and J. Caro, *J. Am. Chem. Soc.,* 2018, **140**, 10094.
[22] Y. Ying, D. Liu, J. Ma, M. Tong, W. Zhang, H. Huang, Q. Yang and C. Zhong, *J. Mater. Chem. A,* 2016, **4**, 13444.
[23] H. Fan, M. Peng, I. Strauss, A. Mundstock, H. Meng and J. Caro, *Nat. Commun.*, 2021, **12**, 38.
[24] R. Li, X. Fu, G. Liu, J. Li, G. Zhou, G. Liu and W. Jin, *J. Membr. Sci.*, 2022, **664**, 121097.
[25] J. Shen, G. Liu, Y. Ji, Q. Liu, L. Cheng, K. Guan, M. Zhang, G. Liu, J. Xiong, J. Yang and W. Jin, *Adv. Funct. Mater.,* 2018, **28**, 1801511.
[26] L. Ding, Y. Wei, L. Li, T. Zhang, H. Wang, J. Xue, L. Ding, S. Wang, J. Caro and Y. Gogotsi, *Nat. Commun.,* 2018, **9**, 155.
[27] Q. Wang, Y. Fan, C. Wu, Y. Jin, C. Li, J. Sunarso, X. Meng and N. Yang, *J. Membr. Sci.,* 2022, **653**, 120533.
[28] R. Wang, J. Qian, X. Chen, Z. Low, Y. Chen, H. Ma, H. Wu, C. M. Doherty, D. Acharya, Z. Xie, M. R. Hill, W. Shen, F. Wang and H. Wang, *Nat. Commun.*, 2023, **14**, 2161.
[29] A. Achari, S. Sahana and M. Eswaramoorthy, *Energy Environ. Sci.*, 2016, **9**, 1224.
[30] D. Wang, Z. Wang, L. Wang, L. Hua and J. Jin, *Nanoscale*, 2015, **7**, 17649.
[31] J. Shen, G. Liu, K. Huang, Z. Chu, W. Jin and N. Xu, *ACS Nano,* 2016, **10**, 3398.
[32] J. Yang, D. Gong, G. Li, G. Zeng, Q. Wang, Y. Zhang, G. Liu, P. Wu, E. Vovk, Z. Peng, X. Zhou, Y. Yang, Z. Liu and Y. Sun, *Adv. Mater.,* 2018, **30**, 1705775.
[33] X. Wang, C. Chi, J. Tao, Y. Peng, S. Ying, Y. Qian, J. Dong, Z. Hu, Y. Gu and D. Zhao, *Chem. Commun.*, 2016, **52**, 8087.